

# Entanglement production in chaotic quantum dots subject to spin-orbit coupling

Diego Frustaglia and Simone Montangero  
*NEST-CNR-INFM & Scuola Normale Superiore, I-56126 Pisa, Italy*

Rosario Fazio  
*NEST-CNR-INFM & Scuola Normale Superiore, I-56126 Pisa, Italy and  
 International School for Advanced Studies (SISSA), I-34014, Trieste, Italy*  
 (Dated: February 8, 2020)

We study numerically the production of orbital and spin entangled states in chaotic quantum dots for non-interacting electrons. A set of attached leads define pairs of orbital and spin qubits. The degree of two-qubit entanglement is quantified by the concurrence. The introduction of spin-orbit coupling permit us to identify signatures of time-reversal symmetry correlations in the entanglement production previously unnoticed, resembling weak-(anti)localization quantum corrections to the conductance. We find the concurrence to be strongly dependent on spin-orbit coupling, showing universal features for broken time-reversal and spin-rotation symmetries.

PACS numbers: 03.67.Mn, 73.23.-b, 05.45.Pq, 71.70.Ej, 72.25.Rb

The possibility of creating entangled quantum states is widely recognized as a fundamental resource for quantum information processing. In solid state physics, several aspects related to the production, control and detection of entangled electronic states have been addressed (see Ref. 1 for a recent review) and different mechanisms have been suggested so far [2, 3, 4, 5, 6, 7, 8, 9, 10, 11, 12, 13, 14, 15, 16, 17, 18, 19, 20, 21, 22]. In contrast to the original belief, it was recently recognized that interaction is not necessary to produce entangled states. Non-interacting particles, initially in a product state, can evolve into an entangled state due to exchange correlations in a scattering process [1, 14, 16, 17, 23]. In this approach the efficiency of the entangler depends on the particular characteristics of the scatterer. Systems of particular interest are disorder-free chaotic quantum dots (chaotic billiards) which allow for a statistical analysis. This case was recently studied by Beenakker *et al.* [14] by means of random-matrix-theory (RMT) approach. They obtained a universal mean value for the degree of two-particle entanglement produced between spatially separated *orbital* channels, and found that this is not significantly affected by the breaking of time-reversal symmetry (TRS). Later, Samuelsson, Sukhorukov, and Büttiker [23] reformulated the problem by formally including the spin, in the absence of any spin-dependent interaction. Here we study the production of both orbital and spin two-particle entanglement for non-interacting electrons in chaotic billiards subject to Rashba spin-orbit (SO) coupling [24]. A numerical approach incorporating the spin-dynamics permit us to go far beyond previous developments, opening additional transport channels contributing to entanglement. Combined with the application of a magnetic flux breaking TRS, we identify the signatures of weak-localization (WL) and weak-antilocalization (WA) corrections to the entanglement production. We find that the production of spin

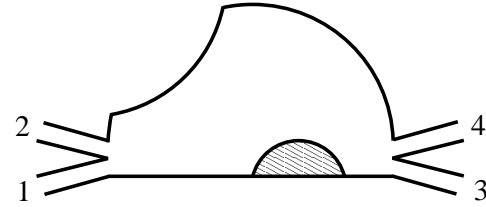


FIG. 1: Chaotic quantum dot entangler used in the numerical model. Leads connected to electron reservoirs support one orbital channel each. The orbital modes support further spin channels.

as well as orbital entanglement is strongly affected by SO coupling on a scale corresponding to the pass from WL to WA. A finite residual entanglement survives after the breaking of both TRS and spin-rotation symmetry showing some universal characteristics.

In our numerical model [25] we consider a two-dimensional chaotic quantum dot connected to electron reservoirs at the left and right as shown in Fig. 1 [26]. Two single-orbital-channel leads are attached at each side of the dot, similar to what proposed in Ref. 14. In addition, each orbital mode can support two spin channels. The SO coupling strength is given in terms of the ratio  $L_{\text{esc}}/L_{\text{SO}}$ , where  $L_{\text{esc}}$  is the classical escape length in an open chaotic billiard and  $L_{\text{SO}}$  is the spin-precession length due to SO coupling. A magnetic flux  $\phi$  (measured in units of the flux quantum  $\phi_0 = hc/e$ ) is produced by a uniform perpendicular magnetic field. Applying a (small) bias voltage between reservoirs produces a coherent electron current passing through the dot from left to right. The single-particle transport properties are characterized by the Landauer-Büttiker linear conductance  $G$ . Coherent backscattering leads to a *minimum* in  $G$  (WL) at  $\phi = 0$  in the absence of SO coupling. For large SO coupling,  $G$  presents a *maximum* (WA) instead [27]. The transition from WL to WA shows up around  $L_{\text{esc}}/L_{\text{SO}} \approx 10$

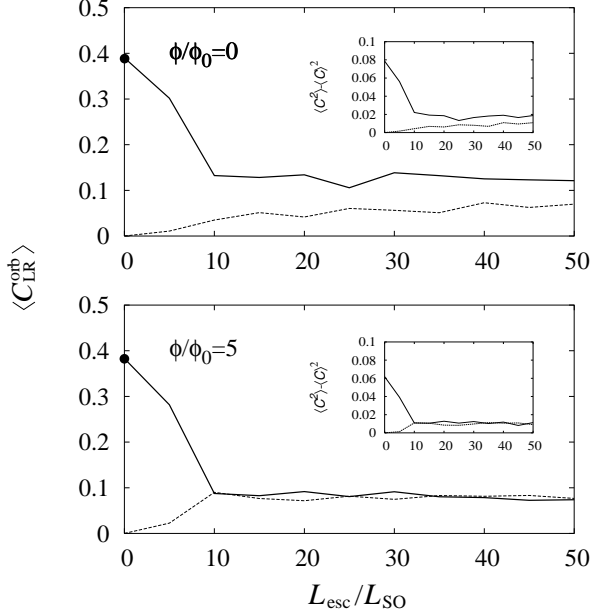


FIG. 2: Left-right orbital entanglement:  $\langle C_{\text{LR}}^{\text{orb}} \rangle$  vs SO coupling with TRS preserved (upper panel) and broken (lower panel). Solid (dashed) lines correspond to (anti)parallel incoming spins. Insets depict the fluctuations, respectively. Full dots: excellent agreement with the only known RMT results up to date [14].

[28]. For a large  $\phi$ , TRS is broken and  $G$  is independent of the SO coupling strength, remaining close to its classical value ( $G_{\text{cl}} = 2e^2/h$  in our case). The crossover from WL to WA also manifest, though differently, in the two-particle entanglement production as we see below.

We calculate the degree of entanglement between pairs of two-level systems or *qubits*, which in our case correspond to an electron leaving the quantum dot in one of two predetermined orbital/spin states. This implies choosing some pairs of outgoing channels of interest, tracing out the nonobserved degrees of freedom compatible with our choice. The two-qubit entanglement is quantified by the concurrence  $0 \leq C \leq 1$  [29], defined as

$$C(\rho) \equiv \max\{0, \lambda_1 - \lambda_2 - \lambda_3 - \lambda_4\}.$$

The  $\lambda_i$ s are the square roots of the eigenvalues (in decreasing order) of the matrix  $\rho\tilde{\rho}$ , where  $\rho \in 4 \times 4$  is a two-qubit density matrix and  $\tilde{\rho} = (\sigma_y \otimes \sigma_y)\rho^*(\sigma_y \otimes \sigma_y)$ , with  $\sigma_y$  the second Pauli matrix. We characterize the production of entanglement in a chaotic dot by calculating the sample-averaged  $\langle C \rangle$  and its fluctuations  $\langle C^2 \rangle - \langle C \rangle^2$ .

We consider a separable (non-entangled) incoming two-particle state of the form

$$|\Psi_{\text{in}}\rangle = |1, s_1\rangle_{\text{in}} |2, s_2\rangle_{\text{in}}. \quad (1)$$

where the ket  $|i, s_i\rangle_{\text{in}}$  represents an incoming particle in lead  $i = 1, 2$  with spin  $s_i = \uparrow, \downarrow$ . The corresponding outgoing state is a coherent superposition of orbital and spin

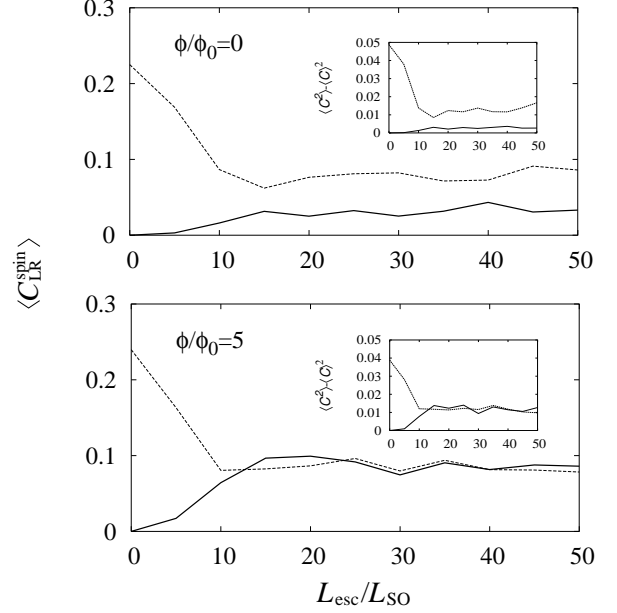


FIG. 3: Left-right spin entanglement:  $\langle C_{\text{LR}}^{\text{spin}} \rangle$  vs. SO coupling with TRS preserved (upper panel) and broken (lower panel). Solid (dashed) lines correspond to (anti)parallel incoming spins. Fluctuations shown in insets.

channel states determined by the single-particle scattering matrix. It reads

$$|\Psi_{\text{out}}\rangle = \sum_{n, \sigma} \sum_{m, \tau} t_{n1}^{\sigma s_1} t_{m2}^{\tau s_2} |n, \sigma\rangle_{\text{out}} |m, \tau\rangle_{\text{out}}, \quad (2)$$

where  $t_{ji}^{ss_i}$  is the generalized quantum amplitude for transmission from the left leads  $i = 1, 2$  with spin  $s_i$  to any lead  $j = 1, \dots, 4$  with spin  $s$ . Amplitudes for outgoing left ( $j = 1, 2$ ) and right ( $j = 3, 4$ ) channels correspond to the reflection and transmission amplitudes, respectively. Importantly, the sum in Eq. (2) does *not* include double-occupancy terms with  $n = m$ ,  $\sigma = \tau$  for the sake of Fermionic statistics.

The outgoing state  $|\Psi_{\text{out}}\rangle$  can be split into three terms with different local particle number at the left ( $n_L$ ) and right ( $n_R$ ) of the dot ( $n_L = 2$ ,  $n_R = 0$ ;  $n_L = 0$ ,  $n_R = 2$ ; and  $n_L = n_R = 1$ ). The accessible entanglement [30] can be studied in each of these terms independently due to local particle number conservation [1]. We investigate first the entanglement between outgoing left and right channels. To this aim we project  $|\Psi_{\text{out}}\rangle$  onto the subspace containing one single excitation at each side of the dot. We obtain

$$|\Psi_{\text{LR}}\rangle = \sum_{p, \alpha} \sum_{q, \beta} (t_{p1}^{\alpha s_1} t_{q2}^{\beta s_2} - t_{q1}^{\beta s_1} t_{p2}^{\alpha s_2}) |p, \alpha\rangle_{\text{L}} |q, \beta\rangle_{\text{R}}, \quad (3)$$

where the indices  $p = 1, 2$ ;  $\alpha = \uparrow, \downarrow$  and  $q = 3, 4$ ;  $\beta = \uparrow, \downarrow$  stand for left and right outgoing channels, respectively. The degree of *orbital entanglement* contained in (3) can

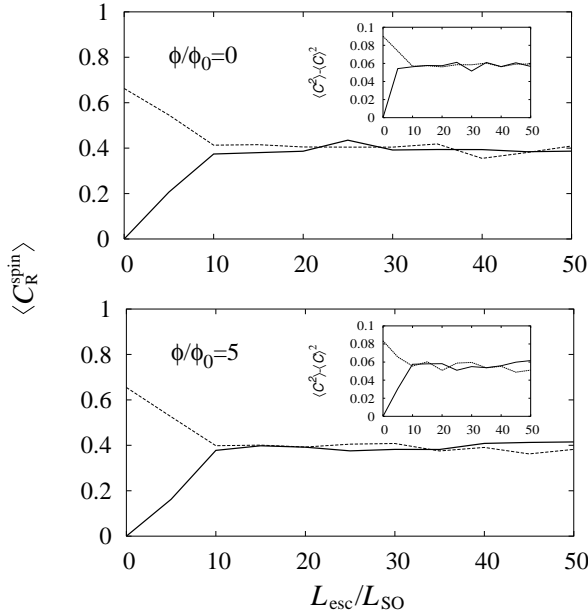


FIG. 4: Transmitted (right) spin entanglement:  $\langle C_R^{\text{spin}} \rangle$  vs. SO coupling with TRS preserved (upper panel) and broken (lower panel). Solid (dashed) lines correspond to (anti)parallel incoming spins. Insets show the fluctuations.

be evaluated by constructing the reduced density matrix (RDM)  $\rho_{\text{LR}}^{\text{orb}} = \sum_{\alpha, \beta} \langle \alpha, \beta | \rho_{\text{LR}} | \alpha, \beta \rangle$  for the two orbital qubits. The Fig. 2 shows results for the average concurrence  $\langle C_{\text{LR}}^{\text{orb}} \rangle$  vs  $L_{\text{esc}}/L_{\text{SO}}$  corresponding to  $\rho_{\text{LR}}^{\text{orb}}$  for parallel ( $s_1 = s_2 = \uparrow$ ; solid line) and antiparallel ( $s_1 = \uparrow, s_2 = \downarrow$ ; dashed line) incoming spins subject to a flux  $\phi$ . The insets depict the fluctuations, respectively. Spins of different species do not contribute to orbital entanglement [23]. This is why only parallel incoming spins show a finite  $\langle C_{\text{LR}}^{\text{orb}} \rangle \approx 0.39$  at  $L_{\text{esc}}/L_{\text{SO}} = 0$  when leaving the quantum dot (full dots in Fig. 2). This value, almost unaffected by the breaking of TRS (finite  $\phi$ ), is in agreement with the only known RMT result [14]. As SO coupling increases, parallel incoming spins suffer spin flipping during transport and outgoing spin channels of different sign open up both at the left and right. This hinders the production of orbital entanglement from originally parallel spins, leading to a reduction of the concurrence. In contrast, for incoming antiparallel spins SO scattering contributes to the formation of orbitally entangled states between spins of the same outgoing species. The scale on which the concurrence varies significantly as a function of  $L_{\text{esc}}/L_{\text{SO}}$  is similar to that determining the transition from WL to WA in the conductance [28]. For large SO coupling, the degree of entanglement saturates as the orientation of outgoing spins randomize. However, a finite difference  $\Delta C \approx 0.05$  survives between curves corresponding to different incoming spin configurations for  $\phi = 0$  (Fig. 2, upper panel). This is a consequence of the TRS corre-

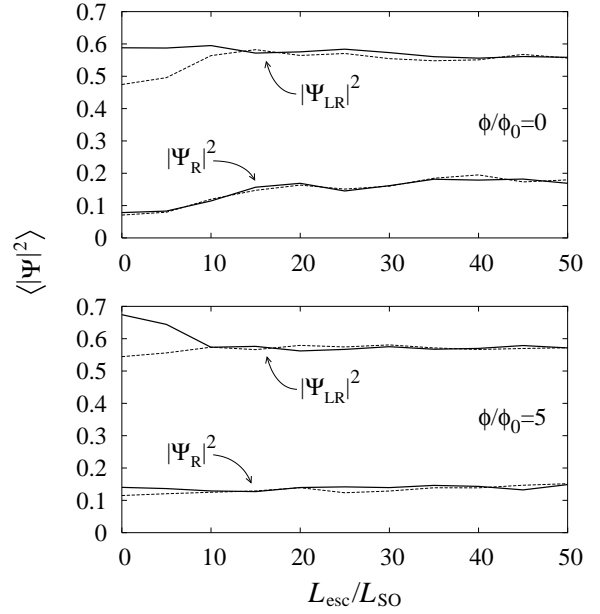


FIG. 5: Sample-averaged probabilities for the states (3) and (4) vs. SO coupling. Upper (lower) panel shows results for preserved (broken) TRS. Solid (dashed) lines correspond to (anti)parallel incoming spins.

lations preserved by the SO interaction. As soon as a finite  $\phi$  breaking TRS is applied the concurrence tends rapidly to a common asymptotic value independent of the initial condition (Fig. 2, lower panel). This indicates that breaking time-reversal and spin-rotation symmetries give rise to a residual orbital entanglement with universal average concurrence  $\langle C_{\text{LR}}^{\text{orb}} \rangle \approx 0.075$  for chaotic dots. We point out that orbital entanglement is very sensitive to the spin dynamics even for broken TRS (Fig. 2, lower panel), where WL and WA quantum corrections to the conductance are absent [27, 28]. Regarding the fluctuations (insets in Fig. 2), they show a functional dependence similar to that of the concurrence. For large  $L_{\text{esc}}/L_{\text{SO}}$ , the standard deviation  $\sqrt{\langle C^2 \rangle - \langle C \rangle^2}$  is of the order of  $\langle C \rangle$ . These features repeat in our results of Figs. 3 and 4. We further note that some difficulties may appear for detecting orbital entanglement produced from incoming antiparallel spins. This is because both incoming as well as outgoing channels would mix at the left side of the dot (unless they can be spatially separated) for the violation of Bell inequalities.

Information regarding *spin entanglement* between left and right channels contained in (3) can be extracted by defining the RDM  $\rho_{\text{LR}}^{\text{spin}} = \sum_{p, q} \langle p, q | \rho_{\text{LR}} | p, q \rangle$  for spin qubits, where this time we trace out the orbital degrees of freedom. Results for the corresponding average concurrence  $\langle C_{\text{LR}}^{\text{spin}} \rangle$  are presented in Fig. 3. In contrast to the previous case of orbital entanglement, antiparallel incoming spins (dashed lines) lead now to a finite

$\langle C_{LR}^{\text{spin}} \rangle$  already at  $L_{\text{esc}}/L_{\text{SO}} = 0$  due to exchange correlations, while parallel incoming spins (solid lines) do not. The presence of multiple orbital channels give rise to an outgoing *mixed* state ( $\text{Tr } \rho_{LR}^{\text{spin}} < 1$ ) with  $\langle C_{LR}^{\text{spin}} \rangle < 1$ . This differs from the case in which *one* single-orbital-channel lead is attached at each side of the quantum dot: there, antiparallel incoming spins would escape at the left and right in a *pure* singlet state with  $\langle C_{LR}^{\text{spin}} \rangle = 1$  independently of the scattering amplitudes (straightforward from Eq. (3); see also Ref. 23). We also note that  $\langle C_{LR}^{\text{spin}} \rangle \ll \langle C_{LR}^{\text{orb}} \rangle$  at  $L_{\text{esc}}/L_{\text{SO}} = 0$  (compare Figs. 2 and 3). This is probably related to the fact that, in contrast to spin entanglement, orbitally entangled electrons leave the dot in a *pure* state ( $\text{Tr } \rho_{LR}^{\text{orb}} = 1$ ). For large SO coupling, Fig. 3 shows features similar to those for orbital entanglement: a finite  $\Delta C$  survives between curves for different incoming states at  $\phi = 0$  due to TRS correlations (Fig. 3, upper panel). The difference disappears as soon as TRS is broken by a finite  $\phi$  (Fig. 3, lower panel). More interestingly, the asymptotic value for  $\langle C_{LR}^{\text{spin}} \rangle$  is very similar to that for  $\langle C_{LR}^{\text{orb}} \rangle$  in Fig. 2 (lower panel). This suggests the existence of a universal value for the concurrence of residual left-right entanglement independently of the initial condition and particular degree of freedom.

We consider now the entanglement production for transmitted spins, i.e., the spin entanglement between channels at the right side of the dot. The transmitted two-particle state can be only *spin-entangled* since there are just two orbital channels (3 and 4) at the right. The projection of the outgoing state (2) onto the subspace with one single excitation on each lead reads

$$|\Psi_R\rangle = \sum_{\alpha, \beta} (t_{31}^{\alpha s_1} t_{42}^{\beta s_2} - t_{41}^{\beta s_1} t_{32}^{\alpha s_2}) |3, \alpha\rangle_R |4, \beta\rangle_R, \quad (4)$$

where  $\alpha$  and  $\beta$  are spin states in the leads 3 and 4, respectively, which play the role of the qubits. After defining  $\rho_R^{\text{spin}} = |\Psi_R\rangle \langle \Psi_R| / \langle \Psi_R | \Psi_R \rangle$ , we plot in Fig. 4 (upper panel) the corresponding  $\langle C_R^{\text{spin}} \rangle$  vs  $L_{\text{esc}}/L_{\text{SO}}$  for  $\phi = 0$ . As in the previous case of left-right spin entanglement, only antiparallel incoming spins (dashed line) lead to a finite  $\langle C_R^{\text{spin}} \rangle$  at  $L_{\text{esc}}/L_{\text{SO}} = 0$ . However, the degree of entanglement is much larger. This holds true also for large SO coupling, where the concurrence arrives at a relatively large common asymptotic value  $\langle C_R^{\text{spin}} \rangle \approx 0.4$  independently of the initial condition. This contrast with our findings for left-right entanglement, where TRS correlations are relevant. The application of a finite  $\phi$ , Fig. 4 (lower panel), does not affect the zero-flux characteristics significantly.

Further information regarding the entanglement production can be extracted from the wave functions (3) and (4) by plotting their modulus square. This is shown in Fig. 5. The larger contribution to the outgoing wave function (2) is given by the left-right component (3) with

probability  $\sim 1/2$ . The transmitted component (4) gives a much smaller contribution instead. This means that highly spin-entangled electrons transmitted to the right are actually produced with a lower probability. This probability increases significantly when breaking TRS for small  $L_{\text{esc}}/L_{\text{SO}}$ . Hence, TRS manifest in the transmitted component (4) only by modifying the production probability without changing the degree of entanglement. We further note in Fig. 5 that a probability difference appears between parallel (solid line) and antiparallel (dashed line) incoming spins in the left-right component due to Fermi statistics. Breaking TRS increases the contribution keeping the relative difference unaffected.

We thank C.W.J. Beenakker and M. Büttiker for useful comments. This work was supported by the EU Spintronics Research Training Network.

---

- [1] C.W.J. Beenakker, cond-mat/0508488.
- [2] P. Recher, E.V. Sukhorukov and D. Loss, Phys. Rev. B **63**, 165314 (2001)
- [3] G.B. Lesovik, T. Martin, G. Blatter, Eur. Phys. J. B **24**, 287 (2001).
- [4] P. Samuelsson, E.V. Sukhorukov, M. Büttiker, Phys. Rev. Lett. **91**, 157002 (2003).
- [5] P. Recher, and D. Loss, Phys. Rev. Lett. **91**, 267003 (2003).
- [6] E. Prada, and F. Sols, Eur. Phys. J. B **40**, 379 (2004).
- [7] P. Samuelsson, E.V. Sukhorukov, and M. Büttiker, Phys. Rev. B **70**, 115330 (2004).
- [8] O. Sauret, D. Feinberg, and T. Martin, cond-mat/0402416.
- [9] P. Recher, and D. Loss. Phys. Rev. B **65**, 165327 (2002).
- [10] C. Bena, S. Vishveshwara, L. Balents, and M.P.A. Fisher, Phys. Rev. Lett. **89**, 037901 (2002).
- [11] V. Bouchiat, N. Chtchelkatchev, D. Feinberg, G.B. Lesovik, T. Martin, J. Torres, Nanotechnology **14**, 77 (2003).
- [12] W.D. Oliver, F. Yamaguchi, and Y. Yamamoto, Phys. Rev. Lett. **88**, 037901 (2002).
- [13] D.S. Saraga, and D. Loss, Phys. Rev. Lett. **90**, 166803 (2003).
- [14] C.W.J. Beenakker, M. Kindermann, C.M. Marcus, and A. Yacoby, *Fundamental Problems of Mesoscopic Physics*, edited by I.V. Lerner, B.L. Altshuler, and Y. Gefen, NATO Science Series II. Vol. 154 (Kluwer, Dordrecht, 2004).
- [15] A.T. Costa and S. Bose, Phys. Rev. Lett. **87**, 277901 (2001).
- [16] C.W.J. Beenakker, C. Emery, M. Kindermann, and J.L. van Velsen, Phys. Rev. Lett. **91**, 147901 (2003).
- [17] P. Samuelsson, E.V. Sukhorukov, and M. Büttiker, Phys. Rev. Lett. **92**, 026805 (2004).
- [18] C.W.J. Beenakker, and M. Kindermann, Phys. Rev. Lett. **92**, 056801 (2004).
- [19] C.W.J. Beenakker, C. Emery, and M. Kindermann, Phys. Rev. B **69**, 115320 (2004).
- [20] P. Samuelsson, and M. Büttiker, Phys. Rev. B **71**, 245317 (2005).

- [21] D.S. Saraga, B.L. Altshuler, D. Loss, and R.M. Westervelt, Phys. Rev. B **71**, 045338 (2005).
- [22] L. Faoro, F. Taddei, and R. Fazio, Phys. Rev. B **69**, 125326 (2004).
- [23] P. Samuelsson, E.V. Sukhorukov, and M. Büttiker, New. J. Phys. **7**, 176 (2005).
- [24] Y. Bychkov and E. Rashba, J. Phys. C **17**, 6039 (1984).
- [25] We implement a recursive Green's function technique based on a tight-binding model. For a detailed description of the method see D. Frustaglia, M. Hentschel, and K. Richter, Phys. Rev. B **69**, 155327 (2004).
- [26] Similar billiards were successfully used in the past for the numerical study of quantum corrections to the conductance of chaotic systems [see H.U. Baranger and P.A. Mello, Phys. Rev. Lett. **73**, 142 (1994)].
- [27] D.M. Zumbühl, J.B. Miller, C.M. Marcus, K. Campman, and A.C. Gossard, Phys. Rev. Lett. **89**, 276803 (2002).
- [28] O. Zaitsev, D. Frustaglia, and K. Richter, Phys. Rev. Lett. **94**, 026809 (2005); *ibid.*, Phys. Rev. B. **72**, 155325 (2005).
- [29] W.K. Wootters, Phys. Rev. Lett. **80**, 2245 (1998).
- [30] H.M. Wiseman and J.A. Vaccaro, Phys. Rev. Lett. **91**, 097902 (2003).